Trailer-Maneuverability in N-Trailer Structures

Maciej Marcin Michałek, *Senior Member, IEEE*

***Abstract*—The letter presents a trailer-maneuverability analysis for the N-trailer kinematic structures comprising a tractor and an arbitrary number of single-axle trailers equipped with steerable or fixed wheels. For an elliptically-shaped set of tractor's input-velocities, we derive a mobility-ellipse generated in a velocity space of the (last) trailer. We show that the on-axle type of hitching present in the N-trailer leads to a singularity of a trailer-mobility (at least one degree of mobility is lost). Furthermore, we provide some relations between kinematic parameters of the N-trailer and its control inputs which enable shaping the trailer-mobility ellipse and decoupling it from a joint-configuration of the vehicle.**

***Index Terms*—Kinematics, nonholonomic mechanisms and systems, wheeled robots, N-trailer, maneuverability.**

I. Introduction

CAPABILITY and dexterity of motion in a task space belong to main characteristics analysed for the robot manipulators, robotic vehicles and devices. These characteristics are represented by the measures of manipulability (defined for manipulators) or maneuverability (defined for mobile robots), which relate to a motion feasibility problem, and can be used for the purposes of optimal motion planning, optimal control, and mechanical design, [1], [2].

Since the first introduction of the fundamental manipulability analysis for serial robot manipulators in [3] (see also [4], [5]), the problems of motion capability and dexterity/agility have been investigated (in the fundamental meaning) for numerous mechanical and robotic systems, like: general constrained multi-body systems [6], underactuated robots and devices [7], single-body wheeled mobile robots [8], mobile manipulators [1], [9], multi-fingered devices [10], continuum robots [11], [12], redundant parallel mechanisms [13], or leader-follower networks [14]. Despite a common usage of the N-trailer structures, and in spite of numerous detailed study concerning their various properties (see, e.g., [15]–[22]), any generic trailer-maneuverability analysis has not been proposed for this kind of multi-body vehicles thus far (some analyses have been made for the tracks with trailers, as in [23], but they address a character/quality of motion in some particular scenarios rather than a generic capability of motion).

A maneuverability analysis seems to be especially important in view of various motion tasks involving agile maneuvering with a trailer [24]. Preserving or shaping a maneuverability is especially important when moving with trailers in a cluttered or narrow environment, where (relatively small) corrections of a trailer motion should be generated only in collision-free (safe) directions, and should not require neither large changes of the N-trailer configuration nor large changes of tractor's velocities. To this purpose, some measures of a trailer-maneuverability can be incorporated as a part of quality/cost criteria used by motion planners and optimal feedback controllers. Therefore, we try to complement a catalogue of maneuverability studies available in the literature by addressing the trailer-maneuverability issue for the N-trailer articulated vehicles comprising a tractor and an arbitrary number of single-axle trailers equipped with steerable or fixed wheels. We investigate how the velocities of a tractor, taken from some prescribed compact subset of an admissible control-input space, can generate a set of velocities of the (last) trailer in the N-trailer chain, and how the dexterity/agility of maneuvering depends on the N-trailer's configuration and its kinematic parameters.

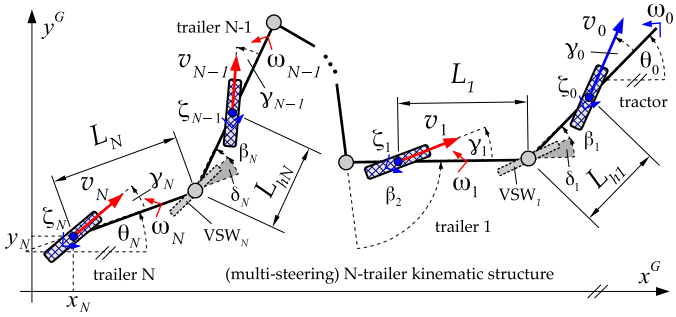

Fig. 1. A single-track kinematic structure of the (multi-steering) N-trailer (only positive hitching offsets L_{hi} are denoted for simplicity); VSW = Virtual Steering Wheel, [19], [25] (note: VSW is not a physical wheel).

Notation: $|\mathcal{I}|$ denotes a cardinality of set $\mathcal{I}$; by $\boldsymbol{Q}^{\dagger} = (\boldsymbol{Q}^{\top}\boldsymbol{Q})^{-1}\boldsymbol{Q}^{\top}$ we understand the left pseudoinverse of matrix $\boldsymbol{Q}$; the substitution operator will be denoted by ':='; where necessary we use a notation: $\mathrm{s}\alpha \equiv \sin\alpha$, $\mathrm{c}\alpha \equiv \cos\alpha$.

II. Prerequisites and Kinematics of N-Trailers

A. Configuration Variables, Inputs, and Basic Relationships

Let us consider a single-track N-trailer kinematic structure comprising a tractor and an arbitrary number of N single-axle trailers, all interconnected by passive rotary joints, as shown in Fig. 1. All the vehicle's segments are treated as rigid bodies in a planar movement, with the wheels rolling without any skid-slip effects. The tractor is a driven segment, with a unicycle-like kinematic control input

$$\boldsymbol{u}_0 \triangleq [\omega_0 \; v_0]^{\top} \in \mathcal{U}_0 \subset \mathbb{R}^2, \tag{1}$$

Manuscript received March 24, 2020; accepted June 24, 2020. Date of publication July 1, 2020; date of current version July 7, 2020. This letter was recommended for publication by Associate Editor Alberto Q. Li and Editor D. Song upon evaluation of the reviewers' comments. This work was supported by the Research Subvention under Grant 0211/SBAD/0911 of the Institute of Automatic Control and Robotics, PUT.

The author is with the Institute of Automatic Control and Robotics (IAR), Poznan University of Technology (PUT), 60-965 Poznań, Poland (e-mail: maciej.michalek@put.poznan.pl).

Digital Object Identifier 10.1109/LRA.2020.3005889

containing an angular velocity ω_0 and a longitudinal velocity v_0 of a mid-point of the tractor's effective wheel. The subset $\mathcal{U}_0$ represents an admissible space of the control input,

$$\boldsymbol{u}_0(t) \in \mathcal{U}_0 \quad \Rightarrow \quad |\omega_0(t)| \leq \omega_{0\mathrm{m}} \ \wedge \ |v_0(t)| \leq v_{0\mathrm{m}}, \tag{2}$$

where the prescribed upper bounds $\omega_{0\mathrm{m}}, v_{0\mathrm{m}} > 0$ determine the maximal admissible velocities of the tractor.

N-trailers are characterized by two kinds of kinematic parameters (see Fig. 1): the trailers' lengths $L_i > 0, i = 1, \ldots, N$, and the hitching offsets $L_{\mathrm{h}i} \in \mathbb{R}$ satisfying $|L_{\mathrm{h}i}| < L_i$ if $L_{\mathrm{h}i} < 0$, while $L_{\mathrm{h}i} > 0$ if the ith rotary joint is located *behind* a wheel's mid-point of the $(i-1)$st vehicle segment, and $L_{\mathrm{h}i} < 0$ if the joint is located *in front* of a wheel's mid-point of the $(i-1)$st segment. In the most general case, the N-trailer can possess both steerable and non-steerable wheels. Let $\mathcal{I}_{\mathrm{S}}$ denote a set of indexes corresponding to steerable wheels. In the special case where all the wheels are non-steerable ($\mathcal{I}_{\mathrm{S}} = \emptyset$), the velocity vector (1) is the only input to the system. In the multi-steering case, [26]–[28], the wheels are independently steerable, thus a vector of steering rates

$$\boldsymbol{u}_{\mathrm{S}} \triangleq [\ldots \zeta_s \ldots]^\top \in \mathcal{U}_{\mathrm{S}} \subset \mathbb{R}^{|\mathcal{I}_{\mathrm{S}}|}, \quad s \in \mathcal{I}_{\mathrm{S}}, \tag{3}$$

is an additional control input of the vehicle, where ζ_s represents a steering rate of the sth steerable wheel (the possible actuated degrees of freedom of the N-trailer have been highlighted in blue in Fig. 1).

In order to describe a configuration of the N-trailer let us introduce the following variables (see [25]):

- steering angles of the steerable wheels: $\gamma_s \in \mathcal{Q}_{\mathrm{S}} \triangleq [-\bar{\gamma}_s; \bar{\gamma}_s]$, $s \in \mathcal{I}_{\mathrm{S}}$, where $\bar{\gamma}_s \in (0; \frac{\pi}{2})$ represents a mechanical bound imposed on a wheel's pivoting motion; for a non-steerable (fixed) wheel $\gamma_j \equiv 0$ and $j \notin \mathcal{I}_{\mathrm{S}}$,
- a pose of the last trailer $\boldsymbol{q}_N \triangleq [\theta_N \, x_N \, y_N]^\top = [\theta_N \, \boldsymbol{p}_N^\top]^\top \in \mathbb{S}^1 \times \mathbb{R}^2$, where θ_N is an orientation angle of the trailer's body, while $\boldsymbol{p}_N$ is a position of a midpoint of its effective wheel,
- joint angles $\beta_i \triangleq (\theta_{i-1} - \theta_i) \in \mathbb{T}, i = 1, \ldots, N$, where θ_i is an orientation of the ith vehicle's segment.

We collect all the variables into the configuration vector

$$\boldsymbol{q} \triangleq [\boldsymbol{\beta}^\top \ \boldsymbol{\gamma}_{\mathrm{S}}^\top \ \boldsymbol{q}_N^\top]^\top \in \mathcal{Q}, \quad \dim(\boldsymbol{q}) = N + |\mathcal{I}_{\mathrm{S}}| + 3, \tag{4}$$

where $\mathcal{Q} = \mathbb{T}^N \times \mathcal{Q}_{\mathrm{S}}^{|\mathcal{I}_{\mathrm{S}}|} \times \mathbb{S}^1 \times \mathbb{R}^2$, $\boldsymbol{\beta} \triangleq [\beta_1 \ \ldots \ \beta_N]^\top$ is a joint-configuration vector, whereas $\boldsymbol{\gamma}_{\mathrm{S}} \triangleq [\ldots \gamma_s \ldots]^\top$ is a vector of steering angles, $\dim(\boldsymbol{\gamma}_{\mathrm{S}}) = |\mathcal{I}_{\mathrm{S}}|$.

Assuming the pure-rolling motion conditions for the vehicle's wheels, one can derive the following velocity transformation valid between any two neighbouring segments for $i = 1, \ldots, N$, (see [21], [25], [27]), that is,

$$\underbrace{\begin{bmatrix}\omega_i \\ v_i\end{bmatrix}}_{\boldsymbol{u}_i} = \underbrace{\begin{bmatrix} -\frac{L_{\mathrm{h}i}}{L_i}\frac{\cos(\beta_i-\gamma_i)}{\cos\gamma_i} & \frac{\sin(\beta_i-\gamma_i+\gamma_{i-1})}{L_i\cos\gamma_i} \\ L_{\mathrm{h}i}\frac{\sin\beta_i}{\cos\gamma_i} & \frac{\cos(\beta_i+\gamma_{i-1})}{\cos\gamma_i}\end{bmatrix}}_{\boldsymbol{J}_i(\beta_i,\gamma_i,\gamma_{i-1})} \underbrace{\begin{bmatrix}\omega_{i-1} \\ v_{i-1}\end{bmatrix}}_{\boldsymbol{u}_{i-1}}. \tag{5}$$

$\boldsymbol{J}_i(\beta_i, \gamma_i, \gamma_{i-1})$ is well defined for all $\beta_i \in \mathbb{T}$ and $\gamma_i \in \mathcal{Q}_{\mathrm{S}}$. The inverse transformation exists for $\gamma_i \in \mathcal{Q}_{\mathrm{S}}$ if $L_{\mathrm{h}i} \neq 0$, namely

$$\boldsymbol{u}_{i-1} = \underbrace{\begin{bmatrix} -\frac{L_i}{L_{\mathrm{h}i}}\frac{\cos(\beta_i+\gamma_{i-1})}{\cos\gamma_{i-1}} & \frac{\sin(\beta_i-\gamma_i+\gamma_{i-1})}{L_{\mathrm{h}i}\cos\gamma_{i-1}} \\ L_i\frac{\sin\beta_i}{\cos\gamma_{i-1}} & \frac{\cos(\beta_i-\gamma_i)}{\cos\gamma_{i-1}}\end{bmatrix}}_{\boldsymbol{J}_i^{-1}(\beta_i,\gamma_i,\gamma_{i-1})} \boldsymbol{u}_i. \tag{6}$$

Using the above basic relationships, one can derive a nonholonomic kinematic model of the N-trailer in the form of driftless dynamics (see [21], [25] for more details)

$$\dot{\boldsymbol{q}} = \boldsymbol{S}(\boldsymbol{q})\boldsymbol{u}, \quad \boldsymbol{u} \triangleq [\boldsymbol{u}_0^\top \ \boldsymbol{u}_{\mathrm{S}}^\top]^\top, \tag{7}$$

which can be decomposed into three subsystems

$$\dot{\boldsymbol{\beta}} = \boldsymbol{S}_\beta(\boldsymbol{\beta}, \boldsymbol{\gamma}_{\mathrm{S}})\boldsymbol{u}_0, \quad \dot{\boldsymbol{\gamma}}_{\mathrm{S}} = \boldsymbol{u}_{\mathrm{S}}, \quad \dot{\boldsymbol{q}}_N = \boldsymbol{S}_N(\boldsymbol{q})\boldsymbol{u}_0, \tag{8}$$

with the kinematic matrices, $\boldsymbol{S}_\beta \in \mathbb{R}^{N\times 2}$ and $\boldsymbol{S}_N \in \mathbb{R}^{3\times 2}$, resulting from the following general forms

$$\begin{bmatrix}\boldsymbol{S}_\beta(\boldsymbol{\beta}, \boldsymbol{\gamma}_{\mathrm{S}}) \\ \hline \boldsymbol{S}_N(\boldsymbol{q})\end{bmatrix} = \left[\begin{array}{c} \boldsymbol{c}^\top\boldsymbol{\Gamma}_1(\beta_1,\gamma_1,\gamma_0) \\ \boldsymbol{c}^\top\boldsymbol{\Gamma}_2(\beta_2,\gamma_2,\gamma_1)\boldsymbol{J}_1(\beta_1,\gamma_1,\gamma_0) \\ \vdots \\ \boldsymbol{c}^\top\boldsymbol{\Gamma}_N(\beta_N,\gamma_N,\gamma_{N-1})\prod_{j=N-1}^{1}\boldsymbol{J}_j(\beta_j,\gamma_j,\gamma_{j-1}) \\ \hline \boldsymbol{G}(\theta_N,\gamma_N)\prod_{j=N}^{1}\boldsymbol{J}_j(\beta_j,\gamma_j,\gamma_{j-1})\end{array}\right], \tag{9}$$

where $\boldsymbol{\Gamma}_j(\beta_j, \gamma_j, \gamma_{j-1}) \triangleq \boldsymbol{I}_{2\times 2} - \boldsymbol{J}_j(\beta_j, \gamma_j, \gamma_{j-1})$, $\boldsymbol{c}^\top \triangleq [1\,0]$, $\boldsymbol{I}_{2\times 2} \in \mathbb{R}^{2\times 2}$ is the identity matrix, while

$$\boldsymbol{G}(\theta_N, \gamma_N) = \begin{bmatrix}1 & 0 & 0 \\ 0 & \cos(\theta_N+\gamma_N) & \sin(\theta_N+\gamma_N)\end{bmatrix}^\top \tag{10}$$

is a matrix of unicycle-like kinematics. For N-trailers with fixed wheels ($\gamma_i \equiv 0$ for all i), the equations (8) reduce to

$$\dot{\boldsymbol{\beta}} = \boldsymbol{S}_\beta(\boldsymbol{\beta})\boldsymbol{u}_0, \qquad \dot{\boldsymbol{q}}_N = \boldsymbol{S}_N(\boldsymbol{q})\boldsymbol{u}_0, \tag{11}$$

where $\boldsymbol{S}_\beta(\boldsymbol{\beta}) \equiv \boldsymbol{S}_\beta(\boldsymbol{\beta}, \boldsymbol{0})$, $\boldsymbol{J}_j(\beta_j, 0, 0) \equiv \boldsymbol{J}_j(\beta_j)$, and $\boldsymbol{q} \triangleq [\boldsymbol{\beta}^\top \ \boldsymbol{q}_N^\top]^\top \in \mathbb{T}^N \times \mathbb{S}^1 \times \mathbb{R}^2$.

Remark 1: One can verify the following properties of the matrix $\boldsymbol{J}_i(\beta_i, \gamma_i, \gamma_{i-1})$ introduced in (5):

P1: $\det \boldsymbol{J}_i = [-L_{\mathrm{h}i}\cos\gamma_{i-1}/(L_i\cos\gamma_i)] < \infty$ for $\gamma_i \in \mathcal{Q}_{\mathrm{S}}$,
P2: $\mathrm{rank}(\boldsymbol{J}_i) \in \{1, 2\}$ for all $\beta_i \in \mathbb{T}$ and $\gamma_i, \gamma_{i-1} \in \mathcal{Q}_{\mathrm{S}}$,
P3: $\mathrm{rank}(\boldsymbol{J}_i) = 1 \Leftrightarrow L_{\mathrm{h}i} = 0$ for $\gamma_i, \gamma_{i-1} \in \mathcal{Q}_{\mathrm{S}}$.

B. Trailer-Maneuverability – Problem Formulation

Without a loss of generality, we will formulate the maneuverability problem for the last (Nth) trailer in a chain.[1] By analogy to the description proposed in [8] for single-body wheeled mobile robots, a kinematic configuration of the Nth trailer with a steerable wheel (i.e., for $N \in \mathcal{I}_{\mathrm{S}}$) can be represented by the vector $\boldsymbol{z}_N \triangleq [\gamma_N \ \boldsymbol{q}_N^\top]^\top$. Now, upon (8)-(9), kinematics of the last trailer can be written as

$$\dot{\gamma}_N = \zeta_N, \tag{12}$$

$$\dot{\boldsymbol{q}}_N = \boldsymbol{S}_N(\boldsymbol{q})\boldsymbol{u}_0 \overset{(5)}{=} \boldsymbol{G}(\theta_N, \gamma_N)\boldsymbol{u}_N, \tag{13}$$

where $\boldsymbol{u}_N \overset{(5)}{=} \prod_{j=N}^{1}\boldsymbol{J}_j(\beta_j, \gamma_j, \gamma_{j-1})\boldsymbol{u}_0$ can be treated as a *virtual input*, which results from an instantaneous transformation

[1]Every ith trailer can be virtually treated as the *last one* if we consider only a sub-chain of the N-trailer comprising a tractor and the first i trailers.

of the tractor input $\boldsymbol{u}_0$ to the velocities of the last trailer along a chain of the N-trailer.

By following [8], let us define for the Nth trailer:

- the *trailer-steerability degree*

$$\Delta_{N\mathrm{s}} \triangleq \begin{cases} 1 & \text{if } N \in \mathcal{I}_{\mathrm{S}} \\ 0 & \text{otherwise} \end{cases},$$

- the *trailer-mobility degree*

$$\Delta_{N\mathrm{m}} \triangleq \operatorname{rank}(\boldsymbol{S}_N(\boldsymbol{q})), \tag{14}$$

- the *trailer-maneuverability degree*

$$\Delta_{N\mathrm{M}} \triangleq \Delta_{N\mathrm{s}} + \Delta_{N\mathrm{m}} \overset{(14)}{=} \Delta_{N\mathrm{s}} + \operatorname{rank}(\boldsymbol{S}_N(\boldsymbol{q})). \tag{15}$$

Since the steering kinematics (12) is independent of the tractor input (moreover, (12) disappears in the case when $N \notin \mathcal{I}_{\mathrm{S}}$), the trailer-steerability degree is constant, and does not depend on the N-trailer's joint-configuration $\boldsymbol{\beta}$. However, the unicycle-like kinematics (13) is driven by the virtual input $\boldsymbol{u}_N$, which is fully dependent on the tractor input $\boldsymbol{u}_0$. Thus, one may expect that the degrees $\Delta_{N\mathrm{m}}$ and $\Delta_{N\mathrm{M}}$ depend, to some extent, on the N-trailer's configuration and/or its kinematic parameters.

In this letter, we investigate how the N-trailer's angular configuration (determined by $\boldsymbol{\beta}$ and $\boldsymbol{\gamma}_{\mathrm{S}}$) and the kinematic parameters, L_i and $L_{\mathrm{h}i}$ $(i = 1, \ldots, N)$, affect the trailer-mobility degree (14), and how they affect a capability of the tractor input $\boldsymbol{u}_0$ to generate velocities of the last trailer in kinematic chains of N-trailers.

III. Trailer-Mobility Analysis for N-Trailers

A. Control-Input Ellipse

Let us introduce the control-input ellipsoid, reduced for $\dim(\boldsymbol{u}_0) = 2$ to the control-input ellipse

$$\boldsymbol{u}_0^{\top} \boldsymbol{M} \boldsymbol{u}_0 = 1, \quad \boldsymbol{M} \triangleq \operatorname{diag}\{\rho, \mu\}, \quad \rho, \mu > 0. \tag{16}$$

We assume that the ellipse (16) is a subset of some admissible input space $\mathcal{U}_0 \subset \mathbb{R}^2$, that is, the semi-axes $\lambda_1 = 1/\sqrt{\rho}$ and $\lambda_2 = 1/\sqrt{\mu}$ satisfy: $\lambda_1 \leq \omega_{0\mathrm{m}}$ and $\lambda_2 \leq v_{0\mathrm{m}}$, see (2). The positive-definite weighting matrix $\boldsymbol{M}$ allows one to account for different units of the components of input vector $\boldsymbol{u}_0$, [4], [29]. In the next subsection, by analogy to the analysis proposed for robotic manipulators in [3] and [30], we will find how the control input ellipse (16) transforms to a trailer-mobility ellipsoid corresponding to a feasible set of the task-space velocities $\dot{\boldsymbol{q}}_N$ of the last trailer.

B. Derivation of a Trailer-Mobility Ellipsoid

According to (13), and assuming that $\operatorname{rank}(\boldsymbol{S}_N(\boldsymbol{q})) = 2$, we can write

$$\boldsymbol{u}_0 \overset{(8)}{=} \boldsymbol{S}_N^{\dagger}(\boldsymbol{q}) \dot{\boldsymbol{q}}_N = [\boldsymbol{S}_N^{\top}(\boldsymbol{q}) \boldsymbol{S}_N(\boldsymbol{q})]^{-1} \boldsymbol{S}_N^{\top}(\boldsymbol{q}) \dot{\boldsymbol{q}}_N. \tag{17}$$

By substituting (17) into the ellipse (16) one gets

$$\boldsymbol{u}_0^{\top} \boldsymbol{M} \boldsymbol{u}_0 \overset{(17)}{=} \dot{\boldsymbol{q}}_N^{\top} \boldsymbol{W}_N \dot{\boldsymbol{q}}_N \overset{(16)}{=} 1, \tag{18}$$

where the matrix $\boldsymbol{W}_N = [\boldsymbol{S}_N^{\dagger}(\boldsymbol{q})]^{\top} \boldsymbol{M} \boldsymbol{S}_N^{\dagger}(\boldsymbol{q}) \in \mathbb{R}^{3\times 3}$ determines the trailer-mobility ellipsoid in the task space. Upon the right-hand side of (17), and recalling that $\boldsymbol{S}_N(\boldsymbol{q}) = \boldsymbol{G}(\theta_N, \gamma_N) \prod_{j=N}^{1} \boldsymbol{J}_j(\beta_j, \gamma_j, \gamma_{j-1})$ (cf. (13) and (9)), one can write (omitting the arguments and introducing $\boldsymbol{H} := \prod_{j=N}^{1} \boldsymbol{J}_j$ for a concise notation)

$$\begin{aligned} \boldsymbol{W}_N &= [\boldsymbol{S}_N^{\dagger}]^{\top} \boldsymbol{M} \boldsymbol{S}_N^{\dagger} = \boldsymbol{S}_N (\boldsymbol{S}_N^{\top} \boldsymbol{S}_N)^{-1} \boldsymbol{M} (\boldsymbol{S}_N^{\top} \boldsymbol{S}_N)^{-1} \boldsymbol{S}_N^{\top} \\ &\overset{(9)}{=} \boldsymbol{G}\boldsymbol{H} (\boldsymbol{H}^{\top} \boldsymbol{G}^{\top} \boldsymbol{G} \boldsymbol{H})^{-1} \boldsymbol{M} (\boldsymbol{H}^{\top} \boldsymbol{G}^{\top} \boldsymbol{G} \boldsymbol{H})^{-1} \boldsymbol{H}^{\top} \boldsymbol{G}^{\top} \\ &= \boldsymbol{G} \boldsymbol{H}^{-\top} \boldsymbol{M} \boldsymbol{H}^{-1} \boldsymbol{G}^{\top} \\ &= \boldsymbol{G} (\boldsymbol{J}_N \ldots \boldsymbol{J}_1 \boldsymbol{M}^{-1} \boldsymbol{J}_1^{\top} \ldots \boldsymbol{J}_N^{\top})^{-1} \boldsymbol{G}^{\top} \qquad (19) \\ &=: \boldsymbol{G} \bar{\boldsymbol{W}}_N^{-1} \boldsymbol{G}^{\top}, \qquad (20) \end{aligned}$$

where the matrix

$$\bar{\boldsymbol{W}}_N(\boldsymbol{\beta}, \boldsymbol{\gamma}_{\mathrm{S}}, \boldsymbol{L}, \boldsymbol{L}_{\mathrm{h}}) \overset{(20)}{:=} \boldsymbol{J}_N \ldots \boldsymbol{J}_1 \boldsymbol{M}^{-1} \boldsymbol{J}_1^{\top} \ldots \boldsymbol{J}_N^{\top} \tag{21}$$

depends, in general, on joint angles, steering angles, and kinematic parameters of the N-trailer, collected here in the vectors $\boldsymbol{L} \triangleq [L_1 \ldots \ L_N]^{\top}$ and $\boldsymbol{L}_{\mathrm{h}} \triangleq [L_{\mathrm{h}1} \ldots \ L_{\mathrm{h}N}]^{\top}$. Upon the result (20), we can rewrite (18) in the form

$$\begin{aligned} \boldsymbol{u}_0^{\top} \boldsymbol{M} \boldsymbol{u}_0 &\overset{(18)}{=} \dot{\boldsymbol{q}}_N^{\top} \boldsymbol{W}_N \dot{\boldsymbol{q}}_N \overset{(20)}{=} \dot{\boldsymbol{q}}_N^{\top} \boldsymbol{G} \bar{\boldsymbol{W}}_N^{-1} \boldsymbol{G}^{\top} \dot{\boldsymbol{q}}_N \\ &\overset{(13)}{=} \boldsymbol{u}_N^{\top} \bar{\boldsymbol{W}}_N^{-1} \boldsymbol{u}_N \overset{(16)}{=} 1. \end{aligned} \tag{22}$$

One concludes that an analysis of the trailer-mobility ellipsoid (18) is equivalent to an analysis of the ellipse represented by (22). Thus, eigenvalues and eigenvectors of matrix (21) determine, respectively, dimensions and an inclination of the trailer-mobility ellipse in the space of velocities $\boldsymbol{u}_N \in \mathcal{U}_N \subset \mathbb{R}^2$.

Remark 2: One can easily verify upon (19) that the matrix $\bar{\boldsymbol{W}}_N$ can be recursively determined by writing

$$\bar{\boldsymbol{W}}_i \triangleq \boldsymbol{J}_i \bar{\boldsymbol{W}}_{i-1} \boldsymbol{J}_i^{\top}, \quad i = 1, \ldots, N, \quad \bar{\boldsymbol{W}}_0 := \boldsymbol{M}^{-1}. \tag{23}$$

By investigating the ellipses $\boldsymbol{u}_i^{\top} \bar{\boldsymbol{W}}_i^{-1} \boldsymbol{u}_i = 1$, for $\boldsymbol{u}_i \triangleq [\omega_i \, v_i]^{\top}$, $i \in \{1, \ldots, N\}$, one can analyse a trailer-mobility for any ith trailer in a kinematic chain of the N-trailer.

C. Trailer-Mobility Measures

To further investigate the trailer-mobility, let us introduce a *trailer-mobility measure* (see [1], [3], [30])

$$\mathcal{M}_N \triangleq \sqrt{\det \bar{\boldsymbol{W}}_N(\boldsymbol{\beta}, \boldsymbol{\gamma}_{\mathrm{S}}, \boldsymbol{L}, \boldsymbol{L}_{\mathrm{h}})}, \tag{24}$$

where the matrix $\bar{\boldsymbol{W}}_N$ results from (21). The measure (24) is proportional to a surface area of the ellipse $\boldsymbol{u}_N^{\top} \bar{\boldsymbol{W}}_N^{-1} \boldsymbol{u}_N = 1$. Following [1], we define an *eccentricity measure*

$$\mathcal{E}_N \triangleq \sqrt{1 - \sigma_{\min}(\bar{\boldsymbol{W}}_N) / \sigma_{\max}(\bar{\boldsymbol{W}}_N)}, \tag{25}$$

where $\sigma_{\min}(\bar{\boldsymbol{W}}_N)$ and $\sigma_{\max}(\bar{\boldsymbol{W}}_N)$ are, respectively, the minimal and maximal singular values of matrix $\bar{\boldsymbol{W}}_N$. The measure (25) is related to an eccentricity of the ellipse $\boldsymbol{u}_N^{\top} \bar{\boldsymbol{W}}_N^{-1} \boldsymbol{u}_N = 1$.

According to the property P1 of matrix $\boldsymbol{J}_i$ (see Remark 1), and upon definition (23) one gets

$$\det \bar{\boldsymbol{W}}_i = (\det \boldsymbol{J}_i)^2 \det \bar{\boldsymbol{W}}_{i-1} = \left(\frac{L_{\mathrm{h}i} \cos \gamma_{i-1}}{L_i \cos \gamma_i} \right)^2 \det \bar{\boldsymbol{W}}_{i-1},$$

which, after its iterative application for $i = 1, \ldots, N$, leads to the trailer-mobility measure for the Nth trailer in the form:

$$\mathcal{M}_N = \prod_{j=1}^{N} \left| \frac{L_{\mathrm{h}j} \cos\gamma_{j-1}}{L_j \cos\gamma_j} \right| \sqrt{\det \boldsymbol{M}^{-1}}$$

$$\stackrel{(16)}{=} \frac{1}{\sqrt{\rho\mu}} \left| \frac{\cos\gamma_0}{\cos\gamma_N} \right| \prod_{j=1}^{N} \frac{|L_{\mathrm{h}j}|}{L_j}. \tag{26}$$

The result (26) deserves some comments.

In contrast to robot manipulators, the trailer-mobility measure $\mathcal{M}_N$ does *not* depend on the joint angles $\boldsymbol{\beta}$, while it only depends on the steering angles γ_0 and γ_N. In the special case of N-trailers with all fixed wheels ($\mathcal{I}_{\mathrm{S}} = \emptyset$), the trailer-mobility measure reduces to

$$\mathcal{M}_N = \frac{1}{\sqrt{\rho\mu}} \prod_{j=1}^{N} \frac{|L_{\mathrm{h}j}|}{L_j}.$$

It should be noted that the independence of $\boldsymbol{\beta}$ obtained for $\mathcal{M}_N$ is valid for the unconstrained joint-kinematics introduced in (8)-(9), where the joint angles can evolve boundlessly ($\boldsymbol{\beta} \in \mathbb{T}^N$). In the case of limited joint angles, the above conclusion is valid locally, i.e., inside an admissible subset of the joint-configuration.

A *distance* to the trailer-mobility singularity $\mathcal{M}_N = 0$ essentially depends on the lengths of hitching offsets present in the N-trailer chain up to the Nth trailer, that is, on $|L_{\mathrm{h}j}|$ for $j = 1, \ldots, N$ (note: $\cos\gamma_0 \neq 0$ for any $\gamma_0 \in \mathcal{Q}_{\mathrm{S}}$). It means that the presence of a single on-axle interconnection in the N-trailer chain before the Nth trailer leads to the singularity $\mathcal{M}_N = 0$. In this context, only the so-called non-Standard N-Trailers, [21], are non-singular.

For a fixed ratio $|\cos\gamma_0 / \cos\gamma_N|$, the trailer-mobility measure $\mathcal{M}_N$ decreases along a chain of the N-trailer with a number of trailers if the ratios $|L_{\mathrm{h}j}|/L_j < 1$ (the most common case for the N-trailer vehicles used in a transportation practice). The above observation may suggest a rough design hint characterized by the rule $|L_{\mathrm{h}i}| = L_i$ for $i = 1, \ldots, N$, in order to preserve the measure $\mathcal{M}_N$ on a sufficiently high level, even in the case of N-trailers with large N. We will return to this issue in Section IV-B.

It is worth noting that the consequences of (26) discussed above stay in agreement with particular quantitative results presented in [31], where the problem of closed-loop sensitivity to input-perturbations was studied. A decrease of the sensitivity, reported in [31] for a shorter hitching offset used in a 1-trailer, results from a lower capability of generating trailer velocities by the tractor inputs, which, in turn, corresponds to a smaller value of measure (26) being proportional to the lengths of hitching offsets.

D. Consequences of $\mathcal{M}_N = 0$ for a Value of Degree Δ_{Nm}

We will show how the singularity $\mathcal{M}_N = 0$ influences the trailer-mobility degree (14). Let us introduce $\boldsymbol{H}^1_N(\boldsymbol{\beta}, \boldsymbol{\gamma}_{\mathrm{S}}) \triangleq \prod_{j=N}^{1} \boldsymbol{J}_j(\beta_j, \gamma_j, \gamma_{j-1})$. First, observe that $\mathrm{rank}(\boldsymbol{G}(\theta_N, \gamma_N)) = 2$ for all $\theta_N \in \mathbb{S}^1$, $\gamma_N \in \mathcal{Q}_{\mathrm{S}}$, see (10). Now, upon (9) and properties of a matrix rank, one concludes: $\mathrm{rank}(\boldsymbol{S}_N(\boldsymbol{q})) = \mathrm{rank}(\boldsymbol{G}(\theta_N, \gamma_N)\boldsymbol{H}^1_N(\boldsymbol{\beta}, \boldsymbol{\gamma}_{\mathrm{S}})) = \mathrm{rank}(\boldsymbol{H}^1_N(\boldsymbol{\beta}, \boldsymbol{\gamma}_{\mathrm{S}})) \in \{0, 1, 2\}$. As a consequence,

$$\Delta_{N\mathrm{m}} \stackrel{(14)}{=} \mathrm{rank}(\boldsymbol{S}_N(\boldsymbol{q})) = \mathrm{rank}(\boldsymbol{H}^1_N(\boldsymbol{\beta}, \boldsymbol{\gamma}_{\mathrm{S}})) \in \{0, 1, 2\}.$$

By recalling (26) and properties P1-P3 from Remark 1, one concludes what follows. If $\forall\, j\ |L_{\mathrm{h}j}| > 0$, then $\mathcal{M}_N > 0$, and $\Delta_{N\mathrm{m}} = \mathrm{rank}(\boldsymbol{H}^1_N(\boldsymbol{\beta}, \boldsymbol{\gamma}_{\mathrm{S}})) = 2$ for all $\boldsymbol{\beta} \in \mathbb{T}^N$, $\boldsymbol{\gamma}_{\mathrm{S}} \in \mathcal{Q}_{\mathrm{S}}^{|\mathcal{I}_{\mathrm{S}}|}$. If there exists a single $|L_{\mathrm{h}j}| = 0$, then $\mathcal{M}_N = 0$ and $\Delta_{N\mathrm{m}} = \mathrm{rank}(\boldsymbol{H}^1_N(\boldsymbol{\beta}, \boldsymbol{\gamma}_{\mathrm{S}})) = 1$. If there exists at least two offsets $|L_{\mathrm{h}j}| = 0$, then $\mathcal{M}_N = 0$ and $\Delta_{N\mathrm{m}} = \mathrm{rank}(\boldsymbol{H}^1_N(\boldsymbol{\beta}, \boldsymbol{\gamma}_{\mathrm{S}})) \leq 1$ (e.g., if $L_{\mathrm{h}i} = L_{\mathrm{h}i-1} = 0$ then $\mathrm{rank}(\boldsymbol{H}^{i-1}_i(\boldsymbol{\beta}^*, \boldsymbol{\gamma}_{\mathrm{S}})) = 0$ at the joint-configuration $\boldsymbol{\beta}^*$ where $\beta^*_{i-1} = \pm\frac{\pi}{2} - \gamma_{i-2}$).

Corollary 1: If $\mathcal{M}_N > 0$ (the regular case) then $\Delta_{N\mathrm{m}} = 2$. If $\mathcal{M}_N = 0$ (the singular case) then $\Delta_{N\mathrm{m}} \leq 1$ (the trailer-mobility degree (14) is decreased at least by one).

A practical meaning of the singularity $\mathcal{M}_N = 0$ can be also explained by referring to an instantaneous motion curvature of the Nth trailer. According to the geometrical interpretation of measure (24), the singularity $\mathcal{M}_N = 0$ corresponds to a situation where the ellipse (22) degenerates to a finite-length line segment in the space $\mathcal{U}_N$ of velocities $\boldsymbol{u}_N = [\omega_N\ v_N]^\top$. A direction of this line segment corresponds to the ratio ω_N/v_N, that is, to a (signed) instantaneous motion curvature κ_N of the N-th trailer. For the sake of simplicity, let us consider the N-trailer with fixed wheels ($\gamma_i \equiv 0$ for all i). In this case, a motion curvature of the ith trailer can be expressed with the so-called *virtual steering angle* δ_i, introduced in [19] and extended in [25], as follows (see Fig. 1)

$$\kappa_i = \frac{1}{L_i} \tan \underbrace{[\beta_i - \arctan(L_{\mathrm{h}i}\kappa_{i-1})]}_{\delta_i} =: f_i(\beta_i, L_{\mathrm{h}i}\kappa_{i-1}),$$

where $\kappa_{i-1} \triangleq \omega_{i-1}/v_{i-1}$ is a curvature of the $(i-1)$st segment of the N-trailer. The angle δ_i is a virtual entity, but it enables expressing the motion curvature κ_i in a similar way as for car-like kinematics. The above recursive formulation for κ_i shows that the curvature of the Nth trailer

$$\kappa_N \triangleq \frac{\omega_N}{v_N} = f_N(\beta_N, L_{\mathrm{h}N} f_{N-1}(\ldots L_{\mathrm{h}2} f_1(\beta_1, L_{\mathrm{h}1}\kappa_0)\ldots))$$

can be *instantaneously* changed by the tractor input $\boldsymbol{u}_0$, *without a change of the joint angles* $\boldsymbol{\beta}$, through $\kappa_0 \triangleq \omega_0/v_0$ only if all the hitching offsets $L_{\mathrm{h}1}, \ldots, L_{\mathrm{h}N}$ are non-zero. This capability corresponds to the trailer-mobility degree equal to 2. However, if at least a single offset $L_{\mathrm{h}i} = 0$ for $i \in \{1, \ldots, N\}$ (leading to the singularity $\mathcal{M}_N = 0$), the change of the curvature κ_N requires a change of the joint angle β_i through an integral relation resulting from (8)-(9). Hence, for $L_{\mathrm{h}i} = 0$, and for the control-input $\boldsymbol{u}_0$ satisfying $\boldsymbol{u}_0^\top \boldsymbol{M} \boldsymbol{u}_0 \leq 1$, a change of a current κ_N to some other value cannot be achieved in an arbitrarily short time interval.

IV. Trailer-Mobility Ellipses for Special Articulated Structures

We are going to illustrate the general result represented by (22), with matrix (21), using some special (yet popular) examples of articulated structures, for which the results of numerical computations can be graphically visualized or which are even analytically tractable. Moreover, we reveal some underlying relations between kinematic parameters of N-trailers and properties of a trailer-mobility ellipse.

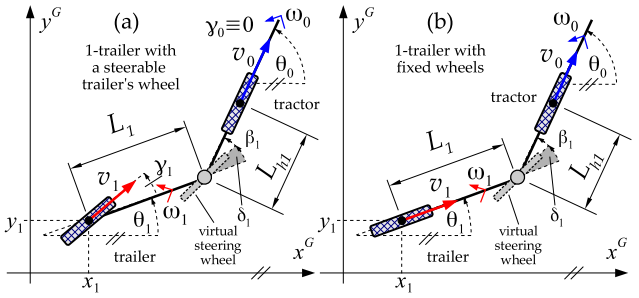

Fig. 2. The single-track kinematic schemes of the 1-trailer structure in two versions: with a steerable trailer's wheel (a) and with fixed wheels (b).

A. Mobility Ellipses for 1-Trailers With a Fixed Tractor's Wheel

For the 1-trailers, it is possible to graphically illustrate trailer-mobility ellipses as a function of the joint angle β_1 or the steering angle γ_1. Let us consider the popular 1-trailer structures ($N = 1$) illustrated in Fig. 2. In the structure in Fig. 2(a), the tractor has a fixed wheel ($\gamma_0 \equiv 0$), whereas the trailer's wheel is steerable. The second structure, presented in Fig. 2(b), is a special case of the former one with the fixed trailer's wheel ($\gamma_1 \equiv 0$). For the 1-trailers from Fig. 2, the general matrix (21) simplifies to

$$\bar{\boldsymbol{W}}_1 \overset{(23)}{=} \boldsymbol{J}_1(\beta_1,\gamma_1,0)\boldsymbol{M}^{-1}\boldsymbol{J}_1^{\top}(\beta_1,\gamma_1,0)$$
$$\overset{(16)}{=} \begin{bmatrix} \frac{L_{\mathrm{h}1}^2\mathrm{c}^2(\beta_1-\gamma_1)}{\rho L_1^2\mathrm{c}^2\gamma_1}+\frac{\mathrm{s}^2(\beta_1-\gamma_1)}{\mu L_1^2\mathrm{c}^2\gamma_1} & \frac{\mathrm{c}\beta_1\mathrm{s}(\beta_1-\gamma_1)}{\mu L_1\mathrm{c}^2\gamma_1}-\frac{L_{\mathrm{h}1}^2\mathrm{s}\beta_1\mathrm{c}(\beta_1-\gamma_1)}{\rho L_1\mathrm{c}^2\gamma_1} \\ \frac{\mathrm{c}\beta_1\mathrm{s}(\beta_1-\gamma_1)}{\mu L_1\mathrm{c}^2\gamma_1}-\frac{L_{\mathrm{h}1}^2\mathrm{s}\beta_1\mathrm{c}(\beta_1-\gamma_1)}{\rho L_1\mathrm{c}^2\gamma_1} & \frac{L_{\mathrm{h}1}^2\mathrm{s}^2\beta_1}{\rho\mathrm{c}^2\gamma_1}+\frac{\mathrm{c}^2\beta_1}{\mu\mathrm{c}^2\gamma_1} \end{bmatrix}. \tag{27}$$

Let us consider some special forms of matrix (27) which can be obtained for particular values of the kinematic parameters L_1 and $L_{\mathrm{h}1}$, especially in the case when the trailer has a fixed (non-steerable) wheel. One can observe that by selecting $|L_{\mathrm{h}1}| := \sqrt{\rho/\mu}$, the matrix (27) reduces to

$$\bar{\boldsymbol{W}}_1(\gamma_1, L_1) = \frac{1}{\mu\mathrm{c}^2\gamma_1}\begin{bmatrix} \frac{1}{L_1^2} & \frac{-\mathrm{s}\gamma_1}{L_1} \\ \frac{-\mathrm{s}\gamma_1}{L_1} & 1 \end{bmatrix}, \tag{28}$$

which does not depend on the joint angle β_1. In this way, a trailer-mobility ellipse can be made invariant with respect to a joint-configuration of the 1-trailer. Furthermore, if the 1-trailer has only fixed wheels (i.e., $\gamma_0 = \gamma_1 \equiv 0$, see Fig. 2(b)), and $|L_{\mathrm{h}1}| := \sqrt{\rho/\mu}$, then the matrix (27) becomes constant and diagonal, $\bar{\boldsymbol{W}}_1 = \mathrm{diag}\{(\mu L_1^2)^{-1}, \mu^{-1}\}$, leading to semi-axes of the ellipse: $\bar{\lambda}_1 = (L_1\sqrt{\mu})^{-1}$, $\bar{\lambda}_2 = \sqrt{\mu^{-1}}$. As a consequence, the trailer-mobility ellipse has its main axes aligned with the axes of the control-input ellipse (16). Now, by selecting the trailer's length $L_1 := \sqrt{\rho/\mu} = |L_{\mathrm{h}1}|$, one gets $\bar{\boldsymbol{W}}_1 = \mathrm{diag}\{\rho^{-1}, \mu^{-1}\} = \boldsymbol{M}^{-1}$, forcing in this way the trailer-mobility ellipse equal to the control-input ellipse (16). Alternatively, by taking $L_1 := 1$, the obtained matrix $\bar{\boldsymbol{W}}_1 = \mu^{-1}\boldsymbol{I}_{2\times 2}$ leads to the *isotropic* trailer-mobility ellipse (a circle) for which $\mathcal{E}_1 = 0$.

It is worth noting that by making a trailer-mobility ellipse configuration-independent, one preserves the same *agility level* (expressed by ranges of achievable velocities and corresponding curvatures of motion) of maneuvering with a trailer for any joint-configuration of an articulated vehicle. It can be used in order to keep sufficiently agile maneuvering in cluttered workspaces, where a vehicle has to continuously adjust its joint-configuration avoiding collisions with surrounding obstacles.

Let us summarize the above analysis in the form of the *design hint* for the 1-trailers with fixed wheels.

Corollary 2 (Design hint): For the prescribed control-input ellipse $\boldsymbol{u}_0^{\top}\boldsymbol{M}\boldsymbol{u}_0 = 1$, with $\boldsymbol{M} = \mathrm{diag}\{\rho, \mu\}$, the special selection of the hitching offset $|L_{\mathrm{h}1}| := \sqrt{\rho/\mu} = \lambda_2/\lambda_1$ for the 1-trailer with fixed wheels, guarantees that all the control inputs satisfying $\boldsymbol{u}_0^{\top}\boldsymbol{M}\boldsymbol{u}_0 \leq 1$ will generate the trailer velocities $\boldsymbol{u}_1$ satisfying $\boldsymbol{u}_1^{\top}\bar{\boldsymbol{W}}_1^{-1}\boldsymbol{u}_1 \leq 1$, with the constant matrix $\bar{\boldsymbol{W}}_1 = \mathrm{diag}\{(\mu L_1^2)^{-1}, \mu^{-1}\}$, *independently* of a value of the joint angle $\beta_1 \in \mathbb{T}$.

Exemplary plots of the ellipses $\boldsymbol{u}_1^{\top}\bar{\boldsymbol{W}}_1^{-1}\boldsymbol{u}_1 = 1$, computed upon (27) for the 1-trailers from Fig. 2, are presented in Fig. 3. The ellipses have been obtained assuming the control-input ellipse (16) with $\boldsymbol{M} := \mathrm{diag}\{1.0, 0.7\}$, changing the joint angle β_1 in the range $[-\frac{\pi}{2}; \frac{\pi}{2}]$, and considering the following three cases of prescribed sets of kinematic parameters and the steering angle of a trailer (cf. (21)): (A) $\bar{\boldsymbol{W}}_1 = \bar{\boldsymbol{W}}_1(\beta_1, 0, 1.0, 0.5)$, (B) $\bar{\boldsymbol{W}}_1 = \bar{\boldsymbol{W}}_1(\beta_1, -\frac{\pi}{4}, 1.0, \sqrt{\rho/\mu})$, and (C) $\bar{\boldsymbol{W}}_1 = \bar{\boldsymbol{W}}_1(\beta_1, -\frac{\pi}{4}, 1.0, 0.005)$. Values of the mobility measure $\mathcal{M}_1 = \sqrt{\det \bar{\boldsymbol{W}}_1(\beta_1, \gamma_1, L_1, L_{\mathrm{h}1})}$ computed for the particular cases are denoted in Fig. 3.

One observes that the mobility ellipses in case (A) are of the same dimensions for all $\beta_1 \in [-\frac{\pi}{2}; \frac{\pi}{2}]$ (the measures $\mathcal{M}_1$ and $\mathcal{E}_1$ are constant). The mobility ellipse, however, rotates as a function of the joint-angle β_1. Furthermore, the steering angle γ_1 affects the eccentricity of the mobility ellipse for different values of the joint angle β_1 – it can be observed in Fig. 4, where we can see a steep degreasing of the measure $\mathcal{E}_1$ for some pairs of angles (β_1, γ_1). Thanks to the special selection of $|L_{h1}| := \sqrt{\rho/\mu}$, the joint-configuration dependency of the mobility ellipse can be avoided, cf. (28). It is shown in case (B), where the mobility ellipses have fixed dimensions and a fixed inclination angle. A value of $\mathcal{E}_1$ depends in this case on the steering angle γ_1 (see the left-hand side plot in Fig. 5), while an inclination angle of the ellipse essentially depends on the parameter L_1 (see the right-hand side plot in Fig. 5). In case (C), the mobility ellipses are almost degenerated to straight-line segments due to a small value of $L_{h1} := 0.005$ m. This is almost a singular case (see the very small value of $\mathcal{M}_1$ presented in Fig. 3), corresponding to the eccentricity measure $\mathcal{E}_1 \approx 1$. The joint-configuration dependency of the ellipse (which rotates with a change of β_1) comes from the same reasons as in case (A).

B. Shaping the Trailer-Mobility Ellipse for N-Trailers With Non-Steerable Wheels by a Selection of Kinematic Parameters

It is possible to use the design hint formulated in Corollary 2 in order to shape a trailer-mobility ellipse for N-trailers equipped with fixed wheels, that is, where $\gamma_i \equiv 0$ for $i = 0, \ldots, N$. In order to obtain the configuration-invariant trailer-mobility ellipse of the last trailer, we will apply the rule from Corollary 2 in a sequential way – from the first to the last trailer.

For the N-trailers with fixed wheels one may derive

$$\bar{\boldsymbol{W}}_1(\beta_1, L_1, L_{\mathrm{h}1}) \overset{(23)}{=} \boldsymbol{J}_1(\beta_1, 0, 0)\boldsymbol{M}^{-1}\boldsymbol{J}_1^{\top}(\beta_1, 0, 0)$$
$$\overset{(16)}{=} \begin{bmatrix} \frac{L_{\mathrm{h}1}^2\mathrm{c}^2\beta_1}{\rho L_1^2}+\frac{\mathrm{s}^2\beta_1}{\mu L_1^2} & \frac{\mathrm{c}\beta_1\mathrm{s}\beta_1}{\mu L_1}-\frac{L_{\mathrm{h}1}^2\mathrm{s}\beta_1\mathrm{c}\beta_1}{\rho L_1} \\ \frac{\mathrm{c}\beta_1\mathrm{s}\beta_1}{\mu L_1}-\frac{L_{\mathrm{h}1}^2\mathrm{s}\beta_1\mathrm{c}\beta_1}{\rho L_1} & \frac{L_{\mathrm{h}1}^2\mathrm{s}^2\beta_1}{\rho}+\frac{\mathrm{c}^2\beta_1}{\mu} \end{bmatrix}.$$

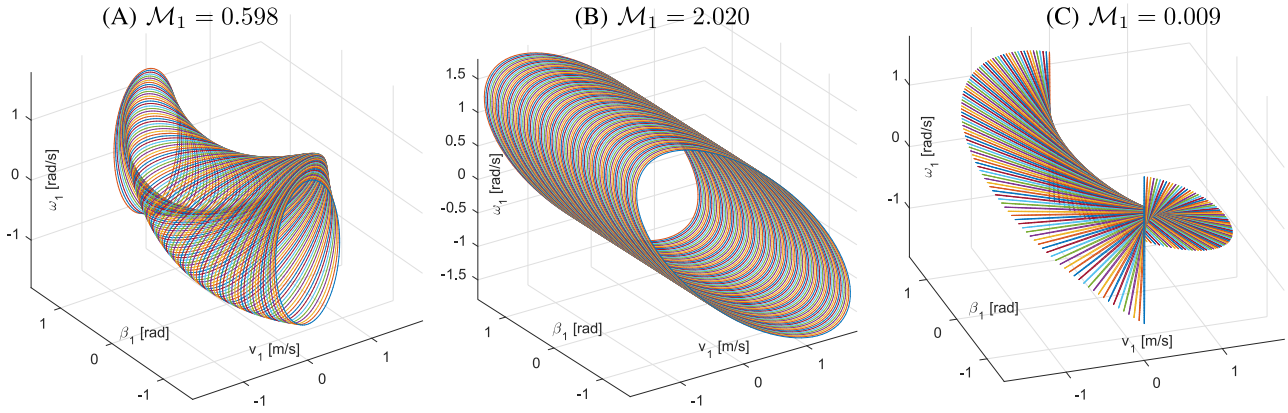

Fig. 3. Exemplary sets of 100 trailer-mobility ellipses $\boldsymbol{u}_1^\top \bar{\boldsymbol{W}}_1^{-1} \boldsymbol{u}_1 = 1$, with matrix $\bar{\boldsymbol{W}}_1 = \bar{\boldsymbol{W}}_1(\beta_1, \gamma_1, L_1, L_{\mathrm{h}1})$ from (27), computed for the 1-trailer in three cases (cf. (21)): (A) with $\bar{\boldsymbol{W}}_1(\beta_1, 0, 1.0, 0.5)$, (B) with $\bar{\boldsymbol{W}}_1(\beta_1, -\frac{\pi}{4}, 1.0, \sqrt{\rho/\mu})$, and (C) with $\bar{\boldsymbol{W}}_1(\beta_1, -\frac{\pi}{4}, 1.0, 0.005)$.

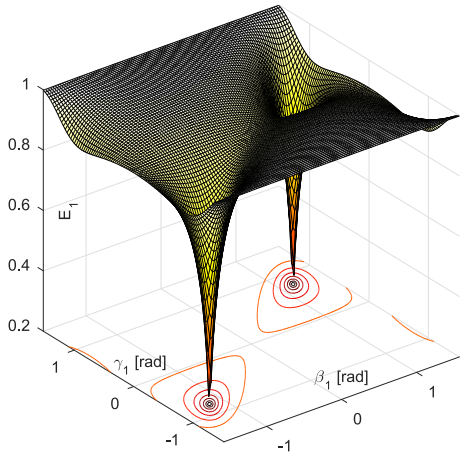

Fig. 4. The eccentricity measure (25) computed for the matrix $\bar{\boldsymbol{W}}_1(\beta_1, \gamma_1, 1.0, 0.5)$ as a function of the joint angle $\beta_1 \in [-\frac{\pi}{2}, \frac{\pi}{2}]$ and the steering angle $\gamma_1 \in [-\frac{\pi}{2} + \epsilon, \frac{\pi}{2} - \epsilon]$ for $\epsilon = 0.05$ rad.

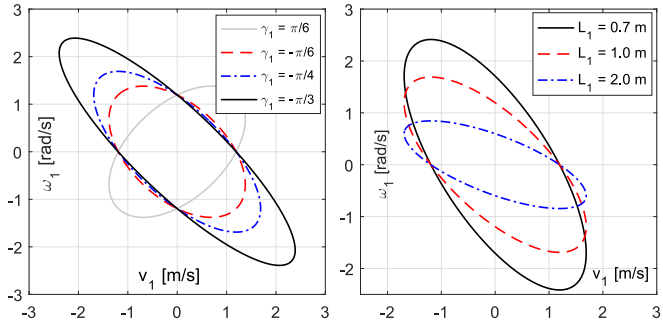

Fig. 5. An influence of the steering angle γ_1 (the left-hand side plots obtained for $L_1 = 1.0$ m) and the trailer's length L_1 (the right-hand side plots obtained for $\gamma_1 = -\frac{\pi}{4}$ rad) on the eccentricity and an inclination of the trailer-mobility ellipse represented by matrix (28) (note: $L_{h1} = \sqrt{\rho/\mu}$).

By taking $|L_{\mathrm{h}1}| := \sqrt{\rho/\mu}$, we get a diagonal matrix $\bar{\boldsymbol{W}}_1 = \mathrm{diag}\{(\mu L_1^2)^{-1}, \mu^{-1}\}$. Using the reduced matrix $\bar{\boldsymbol{W}}_1$, the matrix $\bar{\boldsymbol{W}}_2$ takes the form

$$\bar{\boldsymbol{W}}_2(\beta_2, \boldsymbol{L}, L_{\mathrm{h}2}) \overset{(23)}{=} \boldsymbol{J}_2(\beta_2, 0, 0)\bar{\boldsymbol{W}}_1\boldsymbol{J}_2^\top(\beta_2, 0, 0) = \begin{bmatrix} \frac{L_{\mathrm{h}2}^2 \mathrm{c}^2\beta_2}{\mu L_1^2 L_2^2} + \frac{\mathrm{s}^2\beta_2}{\mu L_2^2} & \frac{\mathrm{c}\beta_2\mathrm{s}\beta_2}{\mu L_2} - \frac{L_{\mathrm{h}2}^2 \mathrm{s}\beta_2\mathrm{c}\beta_2}{\mu L_1^2 L_2} \\ \frac{\mathrm{c}\beta_2\mathrm{s}\beta_2}{\mu L_2} - \frac{L_{\mathrm{h}2}^2 \mathrm{s}\beta_2\mathrm{c}\beta_2}{\mu L_1^2 L_2} & \frac{L_{\mathrm{h}2}^2 \mathrm{s}^2\beta_2}{\mu L_1^2} + \frac{\mathrm{c}^2\beta_2}{\mu} \end{bmatrix},$$

which is decoupled from the first joint angle (i.e., $\bar{\boldsymbol{W}}_2$ does not depend on β_1). Now, by selecting $|L_{\mathrm{h}2}| := L_1$, we get a diagonal matrix for the second trailer, that is, $\bar{\boldsymbol{W}}_2 = \mathrm{diag}\{(\mu L_2^2)^{-1}, \mu^{-1}\}$. As a consequence of the above reasoning, the matrix $\bar{\boldsymbol{W}}_3 = \boldsymbol{J}_3\bar{\boldsymbol{W}}_2\boldsymbol{J}_3^\top = \bar{\boldsymbol{W}}_3(\beta_3, \boldsymbol{L}, L_{\mathrm{h}3})$ will depend only on the third joint angle β_3 (thanks to the decoupling effect of $|L_{\mathrm{h}2}| := L_1$). Continuing the above design procedure, we will obtain constant (configuration-independent) diagonal matrices $\bar{\boldsymbol{W}}_i = \mathrm{diag}\{(\mu L_i^2)^{-1}, \mu^{-1}\}$ for $i = 1, \ldots, N$. Finally, by taking $L_N := \sqrt{\rho/\mu}$ or $L_N := 1$, we get, respectively, $\bar{\boldsymbol{W}}_N = \boldsymbol{M}^{-1}$ (cf. (16)) or $\bar{\boldsymbol{W}}_N = \mu^{-1}\boldsymbol{I}_{2\times 2}$, which lead to the corresponding measures $\mathcal{M}_N = 1/\sqrt{\rho\mu}$ or $\mathcal{M}_N = 1/\mu$.

The trailer-mobility-shaping design procedure proposed above can be summarized by the following design steps:

- S1: take $|L_{\mathrm{h}1}| := \sqrt{\rho/\mu}$ to get $\bar{\boldsymbol{W}}_1 = \mathrm{diag}\{(\mu L_1^2)^{-1}, \mu^{-1}\}$,
- S2: take arbitrary $L_i > 0$ for $i = 1, \ldots, N-1$,
- S3: take $|L_{\mathrm{h}i}| := L_{i-1}$ to get $\bar{\boldsymbol{W}}_i = \mathrm{diag}\{(\mu L_i^2)^{-1}, \mu^{-1}\}$ for $i = 2, \ldots, N$,
- S4: take $L_N := \sqrt{\rho/\mu}$ or $L_N := 1$ to obtain $\bar{\boldsymbol{W}}_N = \boldsymbol{M}^{-1}$ or $\bar{\boldsymbol{W}}_N = \mu^{-1}\boldsymbol{I}_{2\times 2}$, respectively.

It is worth stressing that only the absolute hitching offsets $|L_{\mathrm{h}i}|$ are critical in making the matrices $\bar{\boldsymbol{W}}_i$ independent of $\boldsymbol{\beta}$. In this context, the trailers' lengths can be selected arbitrarily. However, a special selection of the last trailer's length, L_N, enables establishing additional quantitative properties of the trailer-mobility ellipse (see the step S4 above).

C. Shaping the Trailer-Mobility Ellipse by Limiting the Input Domain and Control Scaling

Although the design rules formulated in Sections IV-A and IV-B can be useful in the area of mobile robotics, the design

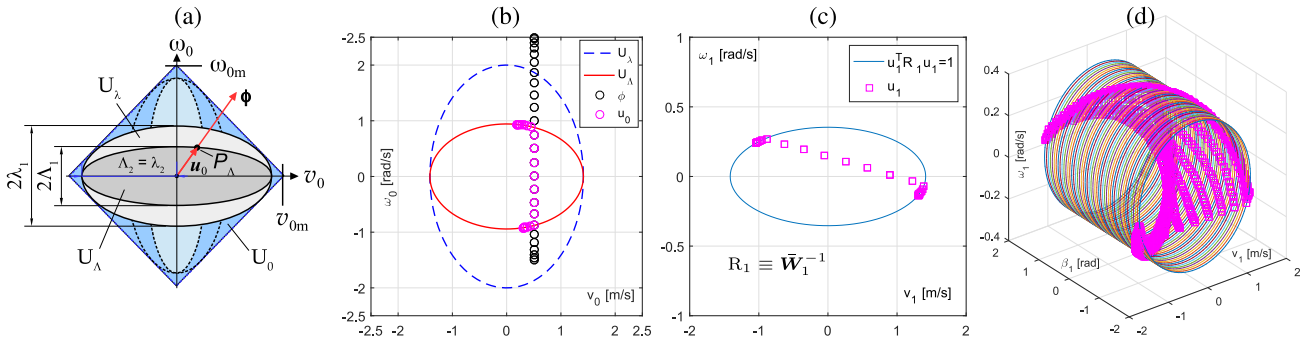

Fig. 6. (a) The largest ellipse $\mathcal{U}_\lambda$ and the sub-ellipse $\mathcal{U}_\Lambda$ as subsets of the admissible control-input space $\mathcal{U}_0$ (alternative ellipses can be defined vertically, as denoted by the dashed lines). (b-d) Exemplary results illustrating an application of scaling procedure (31)-(32) for the subset $\mathcal{U}_\Lambda$ determined upon selection (30) for $\lambda_1 = 2$ rad/s, $\lambda_2 = \sqrt{2}$ m/s, and $L_{\rm h1} = 1.5$ m: (b) the control input ellipses with a set of control samples (precomputed and after scaling), (c) a cross-section (selected for $\beta_1 = \frac{\pi}{3}$ rad) of the set of 100 trailer-mobility ellipses shown in plot (d) obtained for $\beta_1 \in [-\frac{\pi}{2}; \frac{\pi}{2}]$.

decisions for N-trailer structures used in the field of transportation are usually made upon other evidences than the trailer-mobility argument. Note, however, that there exists infinitely many pairs (ρ, μ) leading to the same value of $\sqrt{\rho/\mu}$. Therefore, to still utilize the beneficial effect coming from the equality $|L_{\rm h1}| = \sqrt{\rho/\mu}$, one formulates an alternative *control hint* for the 1-trailers equipped with fixed wheels.

Corollary 3 (Control hint): For *any prescribed* $|L_{\rm h1}| \neq 0$ there exist infinitely many control-input ellipses $\boldsymbol{u}_0^\top \boldsymbol{M}^* \boldsymbol{u}_0 = 1$, with positive definite $\boldsymbol{M}^* = \mathrm{diag}\{\rho^*, \mu^*\}$ of the same semi-axes ratio $\Lambda_2/\Lambda_1 = \sqrt{\rho^*/\mu^*} = |L_{\rm h1}|$ which, for the 1-trailer with fixed wheels, guarantee that all the control inputs satisfying $\boldsymbol{u}_0^\top \boldsymbol{M}^* \boldsymbol{u}_0 \leq 1$ will generate the trailer velocities $\boldsymbol{u}_1$ satisfying $\boldsymbol{u}_1^\top \bar{\boldsymbol{W}}_1^{-1} \boldsymbol{u}_1 \leq 1$ with the matrix $\bar{\boldsymbol{W}}_1 = \mathrm{diag}\{(\mu^* L_1^2)^{-1}, 1/\mu^*\}$, *independently* of a value of the joint angle $\beta_1 \in \mathbb{T}$.

The above hint suggests that one can restrict the control-input ellipse (16) to a sub-ellipse with a ratio of semi-axes $\Lambda_2/\Lambda_1 = |L_{\rm h1}|$, and next constraint the control inputs $\boldsymbol{u}_0$ to this sub-ellipse, in order to obtain a constant and joint-configuration independent trailer-mobility ellipse. Let us consider this possibility in more detail by referring to Fig. 6(a), which illustrates the largest ellipse $\mathcal{U}_\lambda$ (of semi-axes λ_1, λ_2) embedded into an exemplary admissible input space $\mathcal{U}_0 \subset \mathbb{R}^2$. For a 1-trailer with some prescribed non-zero offset $|L_{\rm h1}| \neq \lambda_2/\lambda_1$, we are going to find a subset

$$\mathcal{U}_\Lambda \triangleq \{\boldsymbol{u}_0 : \ \boldsymbol{u}_0^\top \boldsymbol{\Lambda} \boldsymbol{u}_0 \leq 1\}, \quad \boldsymbol{\Lambda} \triangleq \mathrm{diag}\{\Lambda_1^{-2}, \Lambda_2^{-2}\}, \tag{29}$$

which satisfies $\mathcal{U}_\Lambda \subset \mathcal{U}_\lambda$, and $\Lambda_2/\Lambda_1 = |L_{\rm h1}|$. The set $\mathcal{U}_\Lambda$ can be found in different ways, for example, by employing the following (conservative) selection:

$$\begin{cases} \Lambda_1 := \min\{\lambda_1, \lambda_2\}, \ \Lambda_2 := \Lambda_1 |L_{h1}| & \text{if } |L_{h1}| \leq 1, \\ \Lambda_2 := \min\{\lambda_1, \lambda_2\}, \ \Lambda_1 := \Lambda_2 / |L_{h1}| & \text{if } |L_{h1}| > 1. \end{cases} \tag{30}$$

Now, we have to ensure that all the control inputs for kinematics (11) belong to the subset $\mathcal{U}_\Lambda$ for all $t \geq 0$. It can be guaranteed by using a simple on-line input scaling procedure described below. Let $\boldsymbol{\phi}(t) = [\phi_\omega \ \phi_v]^\top \in \mathbb{R}^2 \notin \mathcal{U}_\Lambda$ denote a precomputed control vector for a tractor (resulting, e.g., from an application of some prescribed control law). By scaling the precomputed control $\boldsymbol{\phi}(t)$, one can obtain a control input $\boldsymbol{u}_0(t)$ which belongs to subset (29), namely

$$\boldsymbol{u}_0(t) := \xi(t) \boldsymbol{\phi}(t) \quad \Rightarrow \quad \boldsymbol{u}_0(t) \in \mathcal{U}_\Lambda, \tag{31}$$

where the scaling function $\xi(t) \in (0; 1]$ is defined as follows

$$\xi(t) \triangleq \begin{cases} \sqrt{\frac{\Lambda_1^2 \Lambda_2^2}{\phi_v^2(t) \Lambda_1^2 + \phi_\omega^2(t) \Lambda_2^2}} & \text{if } \ \boldsymbol{\phi}^\top(t) \boldsymbol{\Lambda} \boldsymbol{\phi}(t) > 1, \\ 1 & \text{otherwise.} \end{cases} \tag{32}$$

The first condition used in definition (32) results from a location of point P_Λ (shown in Fig. 6(a)), determined by a projection of an instantaneous control vector $\boldsymbol{\phi}(t)$ on the ellipse $\boldsymbol{u}_0^\top \boldsymbol{\Lambda} \boldsymbol{u}_0 = 1$. Note that the scaling procedure (31)-(32) preserves an instantaneous motion curvature of the tractor, i.e., $\omega_0(t)/v_0(t) = \phi_\omega(t)/\phi_v(t)$ for all $\xi(t) \in (0; 1]$.

The exemplary results, presented in Fig. 6 for the 1-trailer with parameters $L_1 = 4.0$ m and $L_{\rm h1} = 1.5$ m, illustrate an application of the input scaling procedure (31)-(32) for the subset $\mathcal{U}_\Lambda$ (denoted by the red solid line in Fig. 6(b)) which was embedded, upon the rules (30), into the largest ellipse $\mathcal{U}_\lambda$ of semi-axes $\lambda_1 = 2$ and $\lambda_2 = \sqrt{2}$ (see the blue ellipse in Fig. 6(b), corresponding to (16) with $\rho = 0.25$ and $\mu = 0.5$). A set of values of the precomputed control vector $\boldsymbol{\phi}(t)$, with the components $\phi_\omega \triangleq [2\sin(0.4\pi t) + 0.5]$ rad/s and $\phi_v \triangleq 0.5$ m/s, has been denoted in Fig. 6(b) by the black circles. The magenta circles represent the corresponding values of input $\boldsymbol{u}_0$ scaled according to procedure (31). Upon Fig. 6(d), one observes that all the trailer velocities $\boldsymbol{u}_1 = \boldsymbol{J}_1(\beta_1, 0, 0)\boldsymbol{u}_0$ (computed for $\beta_1 \in [-\frac{\pi}{2}; \frac{\pi}{2}]$) do not leave a set bounded by the configuration-independent trailer-mobility ellipse $\boldsymbol{u}_1^\top \bar{\boldsymbol{W}}_1^{-1} \boldsymbol{u}_1 = 1$ with matrix $\bar{\boldsymbol{W}}_1 = \mathrm{diag}\{0.125, 2\}$. Figure 6(c) illustrates a single cross-section of the set from Fig. 6(d), obtained for $\beta_1 = \frac{\pi}{3}$.

The control hint stated in Corollary 3 can be extended to N-trailers with fixed wheels. However in this case, the design requirement $|L_{hi}| := L_{i-1}$ for $i = 2, \ldots, N$, stated in Step S3 in Section IV-B, still has to be met to obtain the configuration-independent trailer-mobility ellipses. It is worth pointing out that by employing the input-scaling procedure (31)-(32) one can intentionally limit the velocity $\boldsymbol{u}_i = [\omega_i \ v_i]^\top$ of any ith trailer, $i \in \{1, \ldots, N\}$, to the *prescribed* subset $\boldsymbol{u}_i^\top \bar{\boldsymbol{W}}_i^{-1} \boldsymbol{u}_i \leq 1$ with $\bar{\boldsymbol{W}}_i = \mathrm{diag}\{(\mu^* L_i^2)^{-1}, 1/\mu^*\}$, where μ^* is now a design (limiting) factor determining a size of a resultant ellipse. By restricting $\boldsymbol{u}_i$ to the prescribed subset, one is able to avoid undesirable (risky) maneuvers with a trailer when moving in cluttered workspaces.

V. Conclusion

The main results of the paper can be summarized as follows:

- A trailer-mobility ellipse depends, in general, on joint angles, steering angles, and kinematic parameters of N-trailers.
- It is possible to shape a trailer-mobility ellipse, and make it joint-configuration invariant, by an appropriate selection of kinematic parameters for the N-trailer, and/or by restricting the tractor control-input to an elliptical subset with a ratio of its semi-axes adjusted to a length of the first hitching offset in the N-trailer chain.
- The presence of at least a single on-axle hitching in the N-trailer chain leads to a singularity of a trailer-mobility (a degree of the trailer-mobility is decreased); even in the case of N-trailers equipped solely with off-axle hitches, a distance to the singularity decreases with a number of those preceding hitches for which $|L_{\mathrm{h}i}|/L_i < 1$.

Practical consequences of shaping the trailer-mobility ellipse can be significant, especially in the context of achievable agility, safety, and a minimal control-cost of maneuvers. It is, however, a separate research topic which goes outside a scope of this paper. Moreover, it seems interesting to analyse in what sense the singularity $\mathcal{M}_N = 0$ affects/limits the achievable control performance for the N-trailers with on-axle hitching. The latter problem, although quantitatively addressed to some extent in [31], still requires qualitative investigations and a generalization.

References

[1] B. Bayle, J.-Y. Fourquet, and M. Renaud, "Manipulability of wheeled mobile manipulators: Application to motion generation," *Int. J. Robot. Res.*, vol. 22, no. 7-8, pp. 565–581, 2003.

[2] T. Pardi, V. Ortenzi, C. Fairbairn, T. Pipe, A. M. G. Esfahani, and R. Stolkin, "Planning maximum-manipulability cutting paths," *IEEE Robot. Autom. Lett.*, vol. 5, no. 2, pp. 1999–2006, Apr. 2020.

[3] T. Yoshikawa, "Manipulability of robotic mechanisms," *Int. J. Robot. Res.*, vol. 4, no. 2, pp. 3–9, 1985.

[4] K. L. Doty, C. Melchiorri, E. M. Schwartz, and C. Bonivento, "Robot manipulability," *IEEE Trans. Robot. Autom.*, vol. 11, no. 3, pp. 462–468, Jun. 1995.

[5] L. Rozo, N. Jaquier, S. Calinon, and D. G. Caldwell, "Learning manipulability ellipsoids for task compatibility in robot manipulation," in *Proc. IEEE/RSJ Int. Conf. Intell. Robots Syst.*, Vancouver, Canada, 2017, pp. 3183–3189.

[6] J. T.-Y. Wen and L. S. Wilfinger, "Kinematic manipulability of general constrained rigid multibody systems," *IEEE Trans. Robot. Autom.*, vol. 15, no. 3, pp. 558–567, Jan. 1999.

[7] D. Prattichizzo, M. Malvezzi, M. Gabiccini, and A. Bicchi, "On the manipulability ellipsoids of underactuated robotic hands with compliance," *Robot. Auton. Syst.*, vol. 60, no. 3, pp. 337–346, 2012.

[8] G. Campion, G. Bastin, and B. d'Andrea Novel, "Structural properties and clasification of kinematic and dynamic models of wheeled mobile robots," *IEEE Trans. Robot. Autom.*, vol. 12, no. 1, pp. 47–62, Feb. 1996.

[9] K. Tchoń and R. Muszyński, "Instantaneous kinematics and dexterity of mobile manipulators," in *Proc. IEEE Int. Conf. Robot. Autom.*, 2000, pp. 2493–2498.

[10] Y. Yokokohji, J. S. Martin, and M. Fujiwara, "Dynamic manipulability of multifingered grasping," *IEEE Trans. Robot.*, vol. 25, no. 4, pp. 947–954, Aug. 2009.

[11] M. Khadem, L. da Cruz, and C. Bergeles, "Force/velocity manipulability analysis for 3D continuum robots," in *Proc. IEEE/RSJ Int. Conf. Intell. Robots Syst.*, Madrid, Spain, 2018, pp. 4920–4926.

[12] L. Wu, R. Crawford, and J. Roberts, "Dexterity analysis of three 6-DOF continuum robots combining concentric tube mechanisms and cable-driven mechanisms," *IEEE Robot. Autom. Lett.*, vol. 2, no. 2, pp. 514–521, Apr. 2017.

[13] N. Baron, A. Philippides, and N. Rojas, "On the false positives and false negatives of the jacobian matrix in kinematically redundant parallel mechanisms," *IEEE Trans. Robot.*, vol. 36, no. 3, pp. 951–958, Jun. 2020.

[14] H. Kawashima and M. Egerstedt, "Manipulability of leader-follower networks with the rigid-link approximation," *Automatica*, vol. 50, no. 3, pp. 695–706, 2014.

[15] J. P. Laumond, "Controllability of a multibody mobile robot," *IEEE Trans. Robot. Autom.*, vol. 9, no. 6, pp. 755–763, Dec. 1993.

[16] P. Rouchon, M. Fliess, J. Levine, and P. Martin, "Flatness, motion planning and trailer systems," in *Proc. 32nd Conf. Decis. Control*, 1993, pp. 2700–2705.

[17] F. Jean, "The car with N trailers: Characterisation of the singular configurations," *ESAIM: COCV*, vol. 1, pp. 241–266, 1996.

[18] A. Bellaiche, F. Jean, and J. J. Risler, "Geometry of nonholonomic systems," in *Robot Motion Planning and Control*, J. P. Laumond, Ed. Berlin, Germany: Springer, 2000, ch. 2, pp. 54–91.

[19] C. Altafini, "Some properties of the general n-trailer," *Int. J. Control*, vol. 74, no. 4, pp. 409–424, 2001.

[20] S.-J. Li and W. Respondek, "Flat outputs of two-input driftless control systems," *ESAIM: COCV*, vol. 18, pp. 774–798, 2012.

[21] M. Michałek, "Non-minimum-phase property of N-trailer kinematics resulting from off-axle interconnections," *Int. J. Control*, vol. 86, no. 4, pp. 740–758, 2013.

[22] I. Duleba, "Kinematic models of doubly generalized n-trailer systems," *J. Intell. Robot. Syst.*, vol. 94, no. 1, pp. 135–142, 2019.

[23] D. Zöbel and C. Weyand, "On the maneuverability of heavy goods vehicles," in *Proc. IEEE Int. Conf. SMC*, 2008, pp. 2303–2308.

[24] M. M. Michałek, "Agile maneuvering with intelligent articulated vehicles: a control perspective," *IFAC PapersOnLine*, vol. 52, no. 8, pp. 458–473, 2019.

[25] M. M. Michałek, "Modular approach to compact low-speed kinematic modelling of multi-articulated urban buses for motion algorithmization purposes," in *Proc. IEEE Intell. Veh. Symp.*, Paris, France, 2019, pp. 1803–1808.

[26] D. Tilbury, O. J. Sördalen, L. Bushnell, and S. S. Sastry, "A multisteering trailer system: Conversion into chained form using dynamic feedback," *IEEE Trans. Robot. Autom.*, vol. 11, no. 6, pp. 807–818, Dec. 1995.

[27] R. Orosco-Guerrero, E. Aranda-Bricaire, and M. Velasco-Villa, "Modeling and dynamic feedback linearization of a multi-steered N-trailer," in *Proc. IFAC 15th Triennial World Congr.*, 2002, pp. 103–108.

[28] O. Ljungqvist and D. Axehill, "A predictive path-following controller for multi-steered articulated vehicles," in *Proc. IFAC World Congr.*, 2020, pp. 1–8.

[29] J. Lachner *et al.*, "The influence of coordinates in robotic manipulability analysis," *Mechanism Mach. Theory*, vol. 146, no. 103722, pp. 1–13, 2020.

[30] L. Sciavicco and B. Siciliano, *Modelling and Control of Robot Manipulators*. Berlin, Germany: Springer-Verlag, 2000.

[31] W. Li, T. Tsubouchi, and S. Yuta, "Manipulative difficulty index of a mobile robot with multiple trailers in pushing and towing with imperfect measurement," in *Proc. IEEE Int. Conf. Robot. Autom.*, 2000, pp. 2264–2269.